Advances in
Geo-Energy Research

Vol. 8, No. 1, p. 61-70, 2023

Original article

Effect of fines migration on oil recovery from carbonate rocks

Abdulmajeed Almutairi[1], Saira Saira[1], Yamin Wang[1,2], Furqan Le-Hussain[1]*

[1]*School of Minerals and Energy Resources Engineering, University of New South Wales, Sydney, NSW 2052, Australia*
[2]*Institute of Energy, Peking University, Beijing 100871, P. R. China*

Keywords:
Carbonate reservoirs
fines migration
permeability decrease
enhanced oil recovery

Cited as:
Almutairi, A., Saira, S., Wang, Y., Le-Hussain, F. Effect of fines migration on oil recovery from carbonate rocks. Advances in Geo-Energy Research, 2023, 8(1): 61-70.
https://doi.org/10.46690/ager.2023.04.06

Abstract:
We perform single-phase and two-phase flooding on Edwards Brown rock samples. The single-phase injection was of seawater or $CaCl_2$ brine, at successive salinities 0.63, 0.21, 0.07, 0.05, and 0 mol/L (distilled water). For $CaCl_2$ brine experimental run, no significant fines migration or permeability decrease is observed. For seawater experimental run, distilled water injection is found to bring about the highest concentration of produced fines and most of the permeability decrease, with the ultimate permeability decrease being 99.94%. Therefore, distilled water injection is used to stimulate fines migration in the following two-phase experimental runs. Two-phase experiments are performed on four Edwards Brown rock samples using seawater or $CaCl_2$ brine as the aqueous phase, and Soltrol® 130 or crude oil as the oleic phase. Rock samples are initially fully saturated with 0.63 mol/L of the selected aqueous solution. This is followed by injecting the selected oil at a constant rate for at least 20 pore volumes to displace brine. Next, selected brine is injected to displace oil, and finally distilled water. For $CaCl_2$ brine, distilled water injection is found to recover no additional oil of either type of oil. However, for seawater, the fines production observed during distilled water injection is found to reduce water relative permeability by two orders of magnitude when Soltrol® 130 is used and by three orders of magnitude when crude oil is used. The seawater experimental runs also brought about additional oil recovery during distilled water injection: 18% when Soltrol® 130 is used and 3.4% when crude oil is used. This last result can be attributed to the plugging of pores due to fines migration, which can divert further injected water into previously unswept pores.

1. Introduction

Low-salinity flooding is known to enhance oil recovery in carbonate reservoirs (Nande and Patwardhan, 2022). The mechanisms of oil recovery during low-salinity flooding are classified as rock-fluid interaction and oil-water interaction (Tetteh et al., 2020). Rock-fluid interaction includes wettability alteration (Mohammadi and Mahani, 2020; Al-Bayati et al., 2022), mineral dissolution (Alotaibi et al., 2018; Mokhtari et al., 2022), multivalent ion exchange (RezaeiDoust et al., 2009; Sheng, 2014), and expansion of the electrical double layer (Brady et al., 2015). Oil-water interaction includes interfacial tension (Mokhtari et al., 2019) and emulsion formation (Sohrabi et al., 2017).

Low-salinity flooding is applied through changing the salinity of injected brine, which is easily implemented and less expensive than other enhanced oil recovery options (Zeinijahromi et al., 2011). Fines migration-induced permeability decrease can be utilized to reduce water mobility (Guo et al., 2023) and hence enhance oil recovery (Zeinijahromi et al., 2011). Fines migration is defined as the release of particles from the rock surface (Moghadasi et al., 2019; Wang et al., 2022). Small fines migrate with the flow, causing blockages or openings of pores and pore throats, which divert the flow and form new pathways (Hussain et al., 2013; Yu et al., 2019; Wang et al., 2021).

Mineral dissolution during water injection can cause the release of fines in sandstone (Fogden et al., 2011; Wang et al., 2021). Lager et al. (2008) asserted that increased Ca concentration and pH of the effluent implies mineral dissolution during water injection. Fines migration and resulting enhanced

Yandy
Scientific
Press

---

*Corresponding author.
E-mail address: a.almutairi@student.unsw.edu.au (A. Almutairi); saira@unsw.edu.au (S. Saira); yamin.wang@pku.edu.cn (Y. Wang); furqan.hussain@unsw.edu.au (F. Le-Hussain).

Received January 20, 2023; revised February 21, 2023; accepted March 13, 2023; available online March 18, 2023.

oil recovery has also been attributed to cation exchange, which weakens the electrostatic force between fines and rock surface (RezaeiDoust et al., 2009; Zhang et al., 2020), and to the dissolution of carbonate minerals (Zahid et al., 2012; Hao et al., 2019).

The extent that fines migration enhances oil recovery in carbonate rocks is unclear. Many studies that listed recovery mechanisms in carbonates omitted fines migration (Yildiz and Morrow, 1996; Jerauld et al., 2008; Lager et al., 2008; Rivet et al., 2010; Katende and Sagala, 2019; Mohammadi and Mahani, 2020). And the studies that did mention fines migration in this context regarded it as insignificant (Zahid et al., 2012; Hao et al., 2019; Tetteh et al., 2020; Zhang et al., 2020; Nande and Patwardhan, 2022).

Zahid et al. (2012) performed water injection on carbonate and chalk samples at room temperature and high temperature. For carbonate, they observed an increase in pressure difference between inlet and outlet at either temperature, but additional oil recovery was observed only at high temperature. Chalk failed to recover additional oil at either temperature (Zahid et al., 2012). The observed increase in pressure difference was attributed to fines migration. The additional oil recovery at high temperature might have been caused by rock mineral dissolution, which was evident from the constant production of Ca in the effluent (Zahid et al., 2012).

Al-Sarihi et al. (2019) found that type of ion can affect fines migration and oil recovery during water injection. They performed water injection on sandstone rock samples by injecting high-salinity brine followed by distilled water. For $CaCl_2$ brine experimental run, they did not observe fines in the effluent. For NaCl brine experimental run, significant fines were mobilized, which diverted fluid flow and enhanced oil recovery in sandstone. However, such experiments have not been conducted on carbonate rocks.

For this work, experimental conditions would preclude previously mentioned mechanisms except for fines migration. The first two experimental runs are single phase with sequentially decreasing salinity, to examine when significant fines migration occurs. The next four experimental runs are two-phase with seawater or $CaCl_2$ brine as the aqueous phase, and Soltrol® 130 or crude oil as the oleic phase. Rock samples are initially fully saturated with 0.63 mol/L brine then oil is injected at a constant rate to displace brine. At least 5 pore volumes (PV) of brine are then injected to displace oil followed by distilled water injection to assess fines migration impact on oil recovery.

2. Materials and methods

The following sections present our experimental setup, rock samples, fluids injected, and the experimental procedure.

2.1 Experimental setup

The equipment used in this study was same as Alumtairi et al. (2022). ISCO 260D syringe pumps were used to inject oil and water into the rock sample. A Hassler coreholder held the rock sample and was mounted horizontally in the injection oven. The horizontal orientation is feasible since the densities of used oil and water are similar. The fluid produced from the coreholder was fed to an AMS-900 two-phase acoustic separator for measuring the volume of recovered fluids. For single-phase experimental runs, the oil pump and separator were not needed. The pressure difference between inlet and outlet was measured by a pressure transducer. The experimental runs were conducted at atmospheric pressure and room temperature (25 °C). Coreholder confining pressure was kept constant at 500 psi.

Table 1. Cylindrical rock sample's injection fluid(s), permeability, and porosity.

Sample	Brine	Oil	Permeability (mD)	Porosity (%)
S1	Seawater	not used	491	41.6
S2	$CaCl_2$	not used	312	43.7
EB1	$CaCl_2$	Soltrol® 130	100.9	41.6
EB2	Seawater	Soltrol® 130	94.7	42.4
EB3	$CaCl_2$	Crude Oil	386.1	45.1
EB4	Seawater	Crude Oil	478.2	42.2

2.2 Rocks

Six Edwards Brown cylindrical rock samples, each having diameter 2.5 cm and length 5 cm, were used in the experimental runs. Edwards Brown is a consolidated carbonate rock obtained from KOCUREK Industries (https://kocurekindustries.com/about-us). A 5 g rock sample was powdered and then subjected to X-Ray Fluorescence (XRF) and X-Ray Powder Diffraction (XRD) analyses, which were used to identify and quantify the mineral composition of the rock samples. The XRD analysis was performed using Empyrean X-ray Diffractometer from PANalytical B. V. HighScore Plus software with an ICDD PDF 4+ data base was used to quantitative interpretation. XRD-XRF analysis show that the rock is composed of Dolomite ($CaMg(CO_3)_2$) 92.6%, Quartz (SiO_2) 6.1%, Calcite ($CaCO_3$) 0.6%, Larnite (Ca_2SiO_4) 0.3%, Calcium aluminium silicate oxide ($Ca_2Al_2SiO_7$) 0.2% and Hatrurite (Ca_3SiO_5) 0.2%.

Each cylindrical rock sample's injection fluid(s), absolute permeability, and porosity are presented in Table 1. The measured porosity and permeability values are similar to those reported by the supplier (https://kocurekindustries.com/carbonates-cores). S identifier in the first column of the table is used for single-phase experiments and EB identifier is used for two-phase experiments.

2.3 Fluids

Milli-Q water was used to prepare different concentrations of seawater and $CaCl_2$ brine. The composition of seawater was taken from Yousef et al. (2012). The composition of seawater was: NaCl 0.54 mol/L, Na_2SO_4 0.034 mol/L, $MgCl_2{\cdot}6H_2O$ 0.03 mol/L, $CaCl_2$ 0.012 mol/L and KCL 0.011 mol/L. The second brine contained only $CaCl_2$ in distilled water. Each cylindrical rock sample was saturated with 0.63 mol/L seawater or $CaCl_2$ brine. For the single-phase experimental runs, injections of the chosen brine were of the following concentrations: 0.63, 0.21 , 0.1, 0.05, and 0 mol/L (distilled water). For two-phase experimental runs, injections of the chosen brine were of the following concentrations: 0.63 and 0 mol/L (distilled water).

Density and viscosity for each brine were determined using a correlation given by El-Dessouky and Ettouney (2002). pH of all fluids was measured using an Oakton pH 700 Benchtop Meter at room temperature (25 °C). Appendix A (see supplementary material) presents composition, density, viscosity, and pH of all injected fluids.

Soltrol® 130 and crude oil were used for the two-phase experimental runs. Soltrol® 130 is a mixture of C_{10} to C_{13} alkanes. The crude oil was composed of 32.95 wt% of C_7 to C_{10}, 49.5 wt% of C_{11} to C_{20}, and 17.55 wt% of $C_{20}+$ components. Asphaltene in the crude oil was negligible (less than 0.05 wt%). Appendix A gives the detailed composition and properties of the crude oil and the properties of Soltrol® 130.

2.4 Experimental procedure

The steps involved depended on whether the experimental run was single-phase or two-phase.

2.4.1 Single-phase experimental run

1) Perform Scanning Electron Microscope (SEM) and Energy Dispersive Spectroscopy (EDS) imaging and analysis on the inlet and outlet faces of the rock sample to record initial condition of pores.
   SEM-EDS was conducted using a Hitachi TM4000Plus SEM operated at 15 keV in standard vacuum mode (30 Pa) with backscattered electron detection, coupled with a Bruker X-Flash 630Hc EDS detector.
2) Measure the rock sample's dry weight.
3) Fully saturate the rock sample with brine and measure the wet weight.
4) Mount the rock sample in the Hassler coreholder.
5) Inject 0.63 mol/L brine at a constant rate of 0.25 cc/min until 30 PV have been injected or the pressure difference between inlet and outlet has stabilized, meaning that the rate of change of pressure difference is less than 0.1 psi/min.
6) Repeat Step 5 for each of 0.21, 0.1, 0.05, and 0 mol/L.
7) Collect effluent every 2 PV injected during Step 5 and 6.
8) Measure the fines concentration of each effluent using a Spectrex Laser Particle Counter PC-2200.
9) Remove the rock sample from the coreholder and weigh it.
10) Dry the rock sample at 60 °C in a drying oven for at least 24 hours, then measure the weight.
11) Perform SEM and EDS imaging and analysis on the inlet and outlet faces of the rock sample to observe any changes at the pore scale.

Inductively Coupled Plasma-Optical Emission Spectrometry (ICP-OES) was performed on selected produced water samples to identify the types and concentrations of dissolved elements. The water samples were divided into two parts; one part was filtered and the other part was treated with acid to dissolve the produced fines. Then ICP-OES analysis was performed on both parts.

2.4.2 Two-phase experimental run

1. Measure rock sample's dry weight.
2. Fully saturate the rock sample with brine and measure its wet weight.
3. Mount the rock sample into the Hassler coreholder.
4. Inject brine at a constant rate of 5 cc/min until the pressure difference between inlet and outlet is stabilized, meaning that the rate of change of pressure difference is less than 0.1 psi/min, to measure absolute permeability.
5. Inject oil at a constant rate of 5 cc/min until at least 20 PV are injected. The oil injection rate is determined as discussed at the end of this section.
6. Inject the chosen brine at a constant rate of 0.25 cc/min for 5 PV. The brine injection rate is determined as discussed at the end of this section.
7. Inject distilled water at a constant rate of 0.25 cc/min until the pressure difference between inlet and outlet is stabilized or the pressure difference reaches the limit of the equipment.
8. During Step 7, collect effluent every 2 cc of volume injected so that the oil produced can be measured.

For oil injection (Step 5), the injection rates are determined based on the capillary to viscous ratio, which is defined as the ratio between the average capillary pressure and the pressure difference across the rock sample at the start of injection (Hussain et al., 2012) as per Eq. (1):

$$\varepsilon=\sigma\frac{A\cos\theta\sqrt{K\varphi}}{\mu_o qL} \tag{1}$$

where ε is the capillary-viscous ratio, σ is the interfacial tension between oil and water, A is the cross-sectional area of the rock sample, θ is the contact angle, K is the rock permeability, φ is the rock porosity, μ_o is the oil viscosity, q is the injection rate, and L is length of the rock sample. For both the Soltrol® 130 and crude oil experimental runs, the injection rate of 5 cc/min yielded ε equal to 0.5 (capillary number is 10^{-5}). At ε equals 0.5 and a capillary number of 10^{-5}, capillary end effects are minimal (Martys et al., 1999; Almutairi et al., 2022). For two-phase brine or water injection, ε was equal to 15 (capillary number is 2.2×10^{-7}) for Soltrol® 130 and 20 (capillary number is 3.3×10^{-7}) for crude oil. Bedrikovetsky et al. (2018) suggested that drag can cause fines migration. Therefore, a lower rate was selected to reduce the effect of drag during two-phase brine or water injection.

3. Results: Single-phase experimental runs

This section presents the permeability changes, pH, produced fines concentration, produced fines composition and concentration of produced dissolved elements for the single-phase experimental runs.

Fig. 1(a) presents the ultimate normalized permeability at each dilution stage. Normalized permeability is the ratio

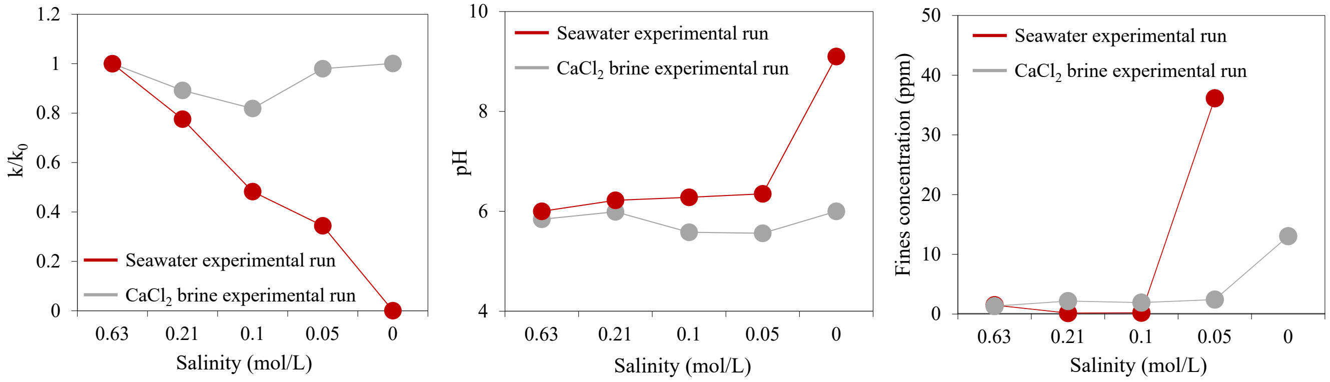

(a) (b) (c)

Fig. 1. Measured results for single-phase experimental runs: (a) Normalized permeability, (b) pH, and (c) produced fines concentration. Each data point presents the stabilized value of the relevant stage.

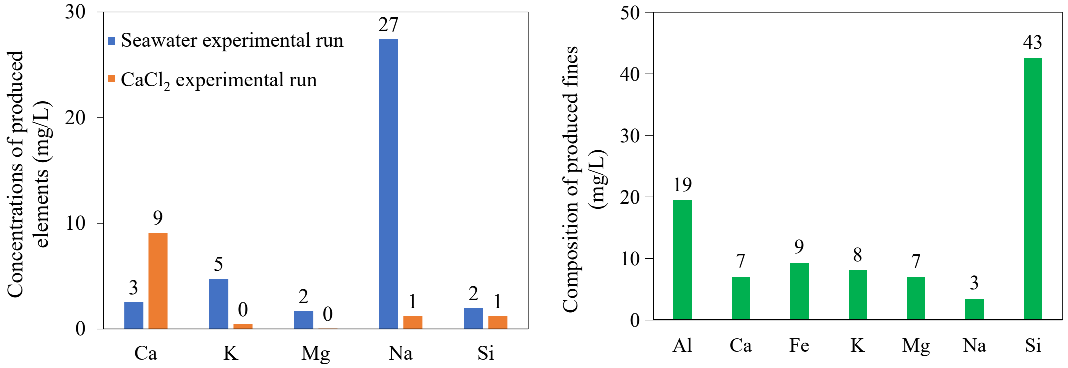

(a) (b)

Fig. 2. (a) Concentration of produced dissolved elements after 10 pore volume injected of distilled water for seawater and $CaCl_2$ experimental runs, (b) composition of produced fines during distilled water injection for sweater experimental run.

of permeability k to initial permeability k_0. For seawater injection, normalized permeability decreased to 78% at the end of 0.21 mol/L salinity injection. At the end of 0.05 mol/L salinity injection, normalized permeability decrease reached 48%. During distilled water injection, normalized permeability dropped significantly to less than 0.1%. For $CaCl_2$ brine injection, permeability decreased down to 82% during 0.21 and 0.1 mol/L salinity injection. During 0.05 mol/L brine injection and distilled water injection, the permeability increased up to the original permeability value.

Fig. 1(b) presents average pH throughout both single-phase experimental runs. pH for both fluids remained close to the pH value of the injected fluid during 0.63 mol/L injection and the diluted brine injections. During distilled water injection in the seawater experimental run, pH increased significantly: up to 9.1. However, during distilled water injection in the $CaCl_2$ brine experimental run, pH remained around 6.

Fig. 1(c) presents fines concentration in the collected effluents. Fines concentration during distilled water injection increased significantly in the seawater experimental run. However, fines concentration during the $CaCl_2$ brine experimental run never exceeded 20 ppm.

Normalized permeability, pH, and produced fines concentration indicated significant fines migration during the seawater experimental run, specifically during 0.05 mol/L brine injection and distilled water injection. pH increase (Fig. 1(b)) and concentration of dissolved elements in the produced water (Fig. 2(a)) confirm mineral reactions. Wang et al. (2022) suggested cation exchange and dissolution reaction occur during water flow in Edwards Brown rock. Examples of cation exchange reaction are:

$$Na^+ + Ca - X_2 \rightarrow Na{-}X + Ca^{2+} \tag{2}$$

$$Na^+ + Mg - X_2 \rightarrow Na - X + Mg^{2+} \tag{3}$$

where X is a mineral surface. Dolomite dissolution is expressed as:

$$CaMg(CO_3)_2 + 2H_2O \rightarrow 2HCO_3{}^- + Ca_2{}^+ + 2CO_3{}^{2-} + Mg^{2+} + 2OH^- \tag{4}$$

Or in the presence of Mg^{2+} ions, the reaction can be:

$$CaMg(CO_3)_2 + Mg^{2+} \rightarrow Ca^{2+} + 2MgCO_3 \tag{5}$$

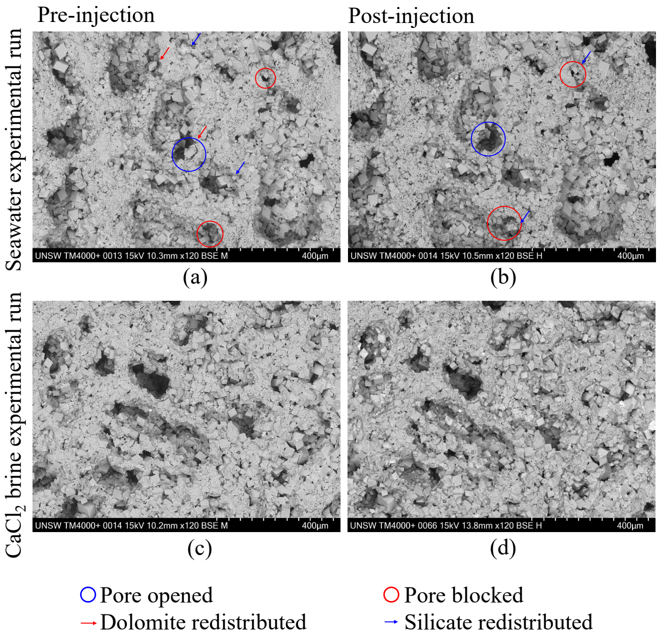

Fig. 3. SEM images pre-injection and post-injection of a portion of the inlet face for each single-phase experimental run. Seawater experimental run images show significant changes post injection (a) and (b) but $CaCl_2$ experimental run images do not show noticeable changes post injection (c) and (d).

Eq. (2) suggests that Na is adsorbed during high salinity injection for seawater experimental run. During distilled water injection, H^+ is adsorbed replacing Na (Lager et al., 2008). As a result, pH is increased and significant Na (27 mg/L) is produced during distilled water injection (Fig. 2(a)). Cation exchange (Eqs. (2) and (3)) did not occur during $CaCl_2$ experimental run due to the absence of monovalent ions in the injected fluid therefore, pH increase during distilled water injection for $CaCl_2$ experimental run is insignificant compared to that during seawater experimental run. Fig. 2(b) indicates that the produced fines during seawater experimental run were predominantly silicates which further indicates that Cation exchange is the main reaction responsible for fines release. Hence no significant fines migration was observed during $CaCl_2$ experimental run and no significant dissolved elements were produced (Fig. 2(a)). Production of dissolved Ca during distilled water injection for $CaCl_2$ experimental run could be due to some dolomite dissolution or desorption of Ca from silicate. An increase in hydroxyl ions (OH^-) from dolomite dissolution (Eq. (5)) can explain the slight increase in pH for $CaCl_2$ experimental run as well as high increase for seawater experimental run during distilled water injection (Chen et al., 2020).

Several studies suggest that when cation exchange reactions are significant (Eqs. (2) and (3)), silicate fines are mobilized which is in agreement with what was observed in the presented experimental runs (Grolimund and Borkovec, 2006; Lebedeva et al., 2009; Gorucu et al., 2019).

Fig. 3 presents pre-injection and post-injection images of a section of the inlet of each single-phase rock sample. More dolomite grains and silicate fines redistribution can be seen in the seawater experimental run than in the $CaCl_2$ brine experimental run. SEM images before and after experiments do not show any visible fractures or other integrity issues.

For seawater experimental run, distilled water injection is found to bring about the highest concentration of produced fines and most of the permeability decrease. Therefore, distilled water injection is used to stimulate fines migration in the following two-phase experimental runs.

4. Results: Two-phase experimental runs

The following subsections present results for the two-phase experimental runs and discuss how they were influenced by fines migration. Section 4.1 presents pressure difference between inlet and outlet results, oil recovery, and produced fines concentration. Section 4.2 presents relative permeability results.

4.1 Pressure difference and oil recovery

During 0.63 mol/L salinity injection for all two-phase experimental runs, oil displacement followed the typical trend observed in literature (Christiansen, 2001). Pressure difference increased until breakthrough but then stabilized because most movable oil had been produced. Oil recovery increased in a straight line until breakthrough, then stabilized. Negligible oil recovery after breakthrough in a laboratory experiment is typical for waterflooding in a strong water wet rock (Bedrikovetsky, 1993). At least 5 PV of brine was injected to ensure that all movable oil was produced and pressure difference was stable. The rest of the text in the subsection only discusses distilled water injection in the experimental runs.

For the $CaCl_2$ brine experimental runs involving either of Soltrol® 130 or crude oil, distilled water injection did not show any additional oil recovery (Figs. 4(c) and 5(c)). As distilled water is injected, it mixes with 0.63 mol/L brine already present in the rock. Since distilled water's viscosity is less, the pressure difference decreases, followed by stabilization when all of the pore space has been filled with distilled water (Figs. 4(a) and 5(a)). Figs. 6(a) and 6(c) present images of an effluent sample collected at 1 PV of distilled water injection for the $CaCl_2$ brine experimental runs. Effluents show only produced water without additional oil production or visible produced fines.

For the experimental runs involving Soltrol® 130, pressure difference increase at the end of distilled water injection was 28 times that at the end of seawater injection. This pressure difference increase was accompanied by high concentration of fines production in effluent. Fig. 6(d) presents an image of an effluent sample collected at 1 PV of distilled water injection. Effluents showed additional oil production and visible produced fines, the latter of which would explain the increase in pressure difference. As the mobilized fines block pores, injected distilled water is diverted to previously unswept pores, thereby displacing additional oil. As a result, 18% additional oil recovery was observed (Fig. 4(d)). The additional oil recovery started after 0.4 PV of distilled water injection (Fig. 4(d)). Additional oil recovery followed a straight line until

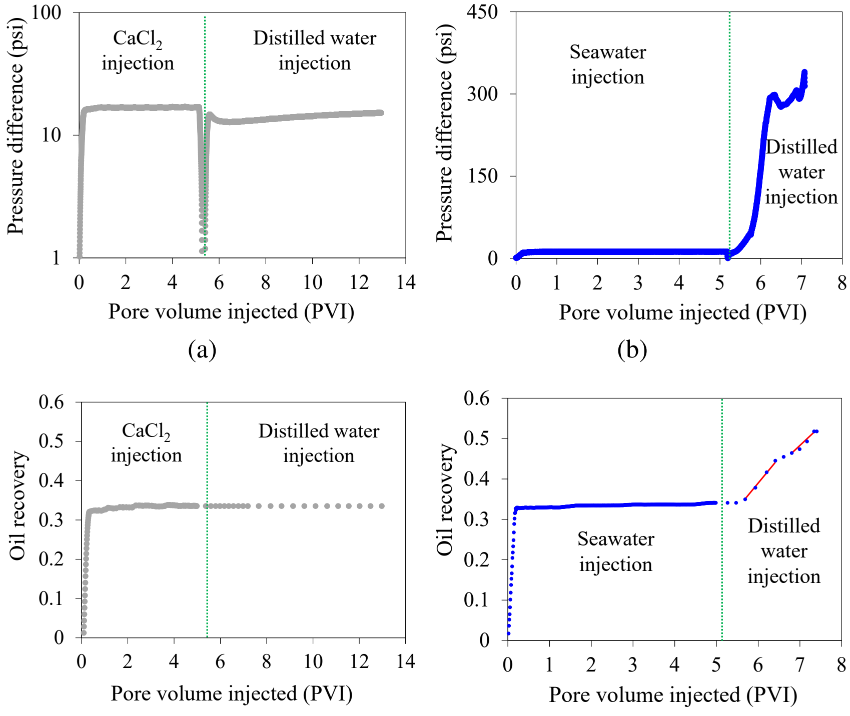

(a) (b)

(c) (d)

Fig. 4. Results for two-phase experimental runs (EB1 in left column, EB2 in right column), starting with the brine injection phase following Soltrol® 130 injection: (a) Imbibition pressure difference for $CaCl_2$ experimental run, (b) imbibition pressure difference for seawater experimental run, (c) imbibition oil recovery for $CaCl_2$ experimental run, and (d) imbibition oil recovery for seawater experimental run. The red line in (d) highlights oil recovery at a constant rate. To more clearly present the data, the vertical axis in (a) depicts a logarithmic scale and a lower maximum value than does the vertical axis in (b).

1.1 PV of distilled water injected (Fig. 4(b)), at which point the pressure difference increased to 300 psi followed by a slight reduction, which was accompanied by a reduction in oil recovery rate. The observed straight-line trend of oil recovery graph suggests that the oil displacement occurred in the form of a bank (Green and Willhite, 1998; Ge et al., 2022). When the oil bank reaches the outlet of the rock sample, oil production starts at a constant rate. Once the tailing end of the oil bank has been produced, pressure difference and oil recovery curves start to stabilize (Bedrikovetsky and Caruso, 2014). However, the pressure difference started to increase again at 1.5 PV of distilled water injection, which coincided with another increase in oil production. At 1.5 PV of distilled water injection, pressure difference resumes increasing due to further pore blockage, leading to further divergence of injected distilled water, which explains the second straight line observed at 1.7 PV of distilled water injection (Fig. 4(d)).

For the experimental runs involving crude oil, pressure difference increase at the end of distilled water injection was 60 times that at the end of seawater injection. This pressure difference increase was accompanied by high concentration of fines production in effluent. Fig. 6(d) presents an image of an effluent sample collected at 1 PV of distilled water injection. Effluents showed additional oil production and visible produced fine. As a result, 3.4% additional oil recovery is observed during distilled water injection (Fig. 5(d)). The additional oil recovery started after 0.9 PV of distilled water injection (Fig. 5(d)). Additional oil recovery followed a straight line until 2.2 PV of distilled water had been injected, after which pressure difference started to stabilize and no more oil was produced (Fig. 6(b)). The discussion in the previous paragraph explains these observations.

Above discussions emphasis on oil recovery induced by fines migration during seawater experimental run. Other mechanisms which could affect oil recovery include: Creation of microfractures due to increased injection pressure, rock deformation due to geochemical changes (Zhang et al., 2019), and wettability alteration due to high pH. Creation of microfractures can affect pores connectivity and oil recovery (Du et al., 2020; Liu et al., 2022). However, SEM images taken at the injection face (where the pressure increase was maximum) did not show any fracturing signs. Our results suggest that most of the reactions involved cation exchanges rather than dissolution which indicate that rock integrity was not compromised. Additionally, both types of oils used in the study do not contain polar components (such as asphaltene) therefore, chances of wettability alteration mechanism are also low. For unconsolidated rocks, grain mobilization may also cause large pressure differences but rocks used in this study were consolidated.

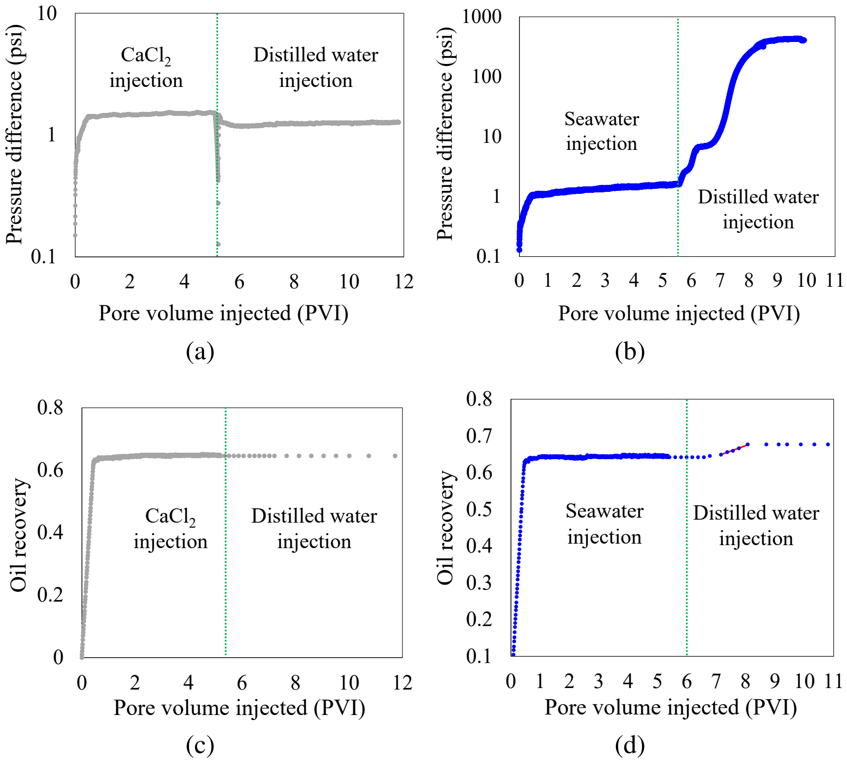

Fig. 5. Results for two-phase experimental runs (EB3 in left column, EB4 in right column), starting with the brine injection phase following crude oil injection: (a) Imbibition pressure difference for $CaCl_2$ experimental run, (b) imbibition pressure difference for seawater experimental run, (c) imbibition oil recovery for $CaCl_2$ experimental run, and (d) imbibition oil recovery for seawater experimental run. The red line in (d) highlights oil recovery at a constant rate. To more clearly present the data, the vertical axis in (a) depicts a logarithmic scale and a lower maximum value than does the vertical axis in (b).

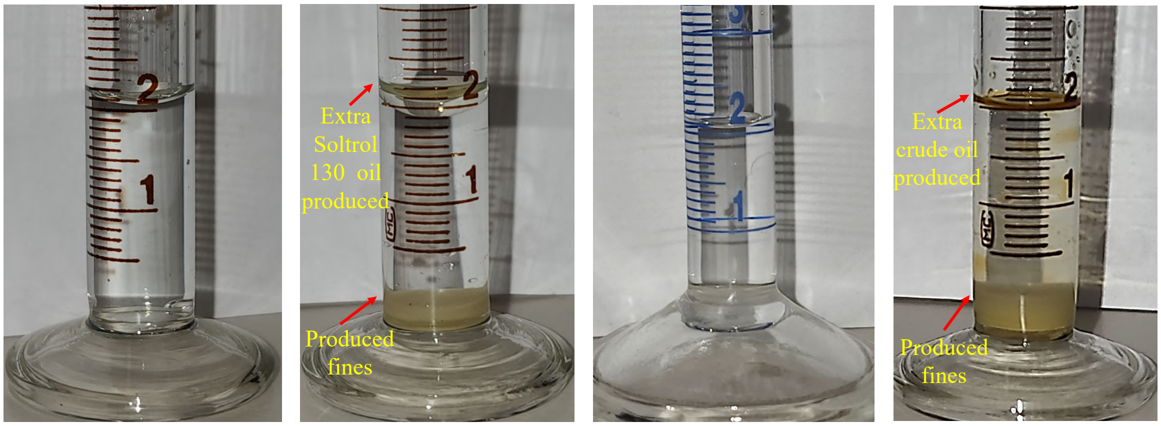

(a) (b) (c) (d)

Fig. 6. Images of effluent samples during distilled water injection following (a) injection of $CaCl_2$ brine to displace Soltrol® 130 (EB1), (b) seawater to displace Soltrol® 130 (EB2), (c) $CaCl_2$ brine to displace crude oil (EB3), and (d) seawater to displace crude oil (EB4). Water produced during seawater experimental run is significantly more turbid indicating large concentration of produced fines.

Table 2. Endpoint saturation and permeability values for all two-phase experimental runs.

Sample	Brine	Oil	S_{wi}	$K_{ro}(S_{wi})$	S_{or_HS}	$K_{rw\_}(S_{or\_HS})$	S_{or_DW}	$K_{rw\_}(S_{or\_DW})$
EB1	$CaCl_2$	Soltrol® 130	0.49	0.850	0.664	0.0301	0.664	0.027
EB2	Seawater	Soltrol® 130	0.49	0.77	0.662	0.047	0.482	0.0016
EB3	$CaCl_2$	Crude Oil	0.318	0.835	0.354	0.106	0.354	0.105
EB4	Seawater	Crude Oil	0.314	0.67	0.358	0.082	0.326	0.00032

4.2 End point relative permeability

Table 2 presents drainage endpoint saturation and permeability for all two-phase experimental runs. Irreducible water saturation (S_{wi}) was the same for drainage of seawater and of $CaCl_2$ brine. Appendix B presents drainage pressure difference and water recovery results, which confirms reproducibility.

For $CaCl_2$ experimental runs, water relative permeability and residual oil saturation after distilled water injection were similar to that after 0.63 mol/L brine injection. However, for seawater experimental runs, distilled water injection brought about a significant decrease in both water relative permeability and residual oil saturation. If seawater injection is taken as a baseline, water relative permeability during distilled water injection was two orders of magnitude lower when Soltrol® 130 was used and three orders of magnitude lower when crude oil was used. In addition, residual oil saturation during distilled water injection was 18% lower when Soltrol® 130 was used and 3.4% lower when crude oil was used. For field-scale applications, the reduction in water relative permeability represents a reduction in water mobility and a reduction in water injectivity. A reduced mobility of the injected fluid is a desirable effect which is known to improve both displacement and sweep efficiencies and therefore improve oil recovery (Green and Willhite, 1998). However, reduced injectivity would cause increased injection cost.

For the seawater experimental run when Soltrol® 130 was involved, residual oil saturation after seawater injection, S_{or_HS}, reached 66.2%, and when crude oil was used, residual oil saturation after seawater injection, S_{or_DW}, reached 35.8%. For the experimental run involving crude oil, higher oil recovery during seawater injection also explains the lower additional oil recovery during distilled water injection. Additionally, type of oil used will affect rock-fluid interactions, which can then influence the pressure difference, water relative permeability, and oil recovery.

5. Conclusion

Single-phase experimental runs were performed to assess the salinity conditions that stimulate fines migration. Results showed that distilled water injection after seawater injection brought about the highest concentration of produced fines. Two-phase experimental runs were also performed, to assess the impact of fines migration on oil recovery from carbonate rocks. For the two-phase experimental runs, oil was displaced by injecting at least 5 pore volumes of 0.63 mol/L of brine, followed by distilled water. The two-phase experimental runs led to the following conclusions:

1) For $CaCl_2$ experimental runs involving either Soltrol® 130 or crude oil, the pressure difference at the end of distilled water injection was similar to that at the end of seawater injection; (2) water relative permeability and residual oil saturation during distilled water injection remained similar to the values during 0.63 mol/L brine injection; and no oil recovery was observed during distilled water injection.

The above observations are attributed to insignificant fines migration during the experimental runs.

2) For seawater experimental runs involving Soltrol® 130, the pressure difference increase at the end of distilled water injection was 28 times that at the end of seawater injection; water relative permeability decreased by two orders of magnitude during distilled water injection; and 18% additional oil recovery was observed during distilled water injection.

Mineral reactions led to mobilization of fines, which can cause pore blockage yielding increased pressure difference and decreased water relative permeability. The pore blockage can divert further injected water into pores containing previously immovable oil, which explains the additional oil recovery.

3) For seawater experimental runs involving crude oil, the pressure difference increase at the end of distilled water injection was 60 times that at the end of seawater injection; water relative permeability decreased by three orders of magnitude during distilled water injection; and 3.4% additional oil recovery was observed during distilled water injection.

The mechanisms involved in the above crude oil experimental runs are same as those involving Soltrol® 130. The different magnitude of pressure difference increase, water relative permeability decrease, and additional oil recovery are attributed to different oil types and the residual oil saturation before distilled water injection.

Reduction in water relative permeability means reduced water mobility and injectivity. Reduction in the mobility of the injected fluid is known as the mobility control method, which enhances oil recovery (Green and Willhite, 1998). However, a decrease of two to three orders of magnitude in injectivity might not be desirable for field-scale applications (Lemon et al., 2011). Nevertheless, the degree of fines migration can be controlled. For instance, if we would have selected 0.05 mol/L salinity to represent low-salinity injection, injectivity loss would have been less. For field applications, experimental runs should be conducted on reservoir rock samples to assess and select the most suitable ions and concentration.

Acknowledgements

The authors acknowledge David H. Levin (Murphy, NC, USA) for editing the manuscript, Saudi Aramco for sponsoring Abdulmajeed Almutairi's PhD studies, and UNSW for providing lab services. The authors acknowledge the facilities and the scientific and technical assistance of Mark Wainwright Analytical Centre (MWAC) at UNSW Sydney.

Supplementary file

https://doi.org/10.46690/ager.2023.04.06

Conflict of interest

The authors declare no competing interest.

References

Al-Bayati, A., Karunarathne, C. I., Al Jehani, A. S., et al. Wettability alteration during low-salinity water flooding. Energy & Fuels, 2022, 36(2): 871-879.

Almutairi, A., Othman, F., Ge, J., et al. Modified johnson-bossler-naumann method to incorporate capillary pressure boundary conditions in drainage relative permeability estimation. Journal of Petroleum Science and Engineering, 2022, 210: 110064.

Alotaibi, M. B., Cha, D., Alsofi, A. M., et al. Dynamic interactions of inorganic species at carbonate/brine interfaces: An electrokinetic study. Colloids and Surfaces A: Physicochemical and Engineering Aspects, 2018, 550: 222-235.

Al-Sarihi, A., Russell, T., Bedrikovetsky, P., et al. Fines stabilization by ca ions and its effect on lsw injection. Energy & Fuels, 2019, 33(11): 10775-10786.

Bedrikovetsky, P. Mathematical Theory of Oil and Gas Recovery: With Applications to Ex-ussr Oil and Gas Fields. Dordrecht, Netherlands, Kluwer Academic Publishers, 1993.

Bedrikovetsky, P., Caruso, N. Analytical model for fines migration during water injection. Transport in Porous Media, 2014, 101(2): 161-189.

Bedrikovetsky, P., Zeinijahromi, A., Badalyan, A., et al. Prediction and management of fines migration for oil and gas production. Вести газовой науки, 2018, 5(37): 192-200.

Brady, P. V., Morrow, N. R., Fogden, A., et al. Electrostatics and the low salinity effect in sandstone reservoirs. Energy & Fuels, 2015, 29(2): 666-677.

Chen, Y., Ubaidah, A., Elakneswaran, Y., et al. Detecting ph and Ca^{2+} increase during low salinity waterflooding in carbonate reservoirs: Implications for wettability alteration process. Journal of Molecular Liquids, 2020, 317: 114003.

Christiansen, R. L. Two-phase Flow Through Porous Media: Theory, Art and Reality of Relative Permeability and Capillary Pressure. R. L. Christiansen, Golden, Colo., 2001.

Du, Y., Mehmani, A., Xu, K., et al. Microfluidic diagnostics of the impact of local microfracture connectivity on hydrocarbon recovery following water injection. Water Resources Research, 2020, 56(7): e2019WR026944.

El-Dessouky, H. T., Ettouney, H. M. Fundamentals of Salt Water Desalination. Amsterdam, Netherlands, Elsevier Science B. V., 2002.

Fogden, A., Kumar, M., Morrow, N. R., et al. Mobilization of fine particles during flooding of sandstones and possible relations to enhanced oil recovery. Energy & Fuels, 2011, 25(4): 1605-1616.

Ge, J., Saira, Smith, B., et al. Laboratory comparison of tertiary N_2, CH_4, and CO_2 injection into an inland oil field sample. Fuel, 2022, 324: 124635.

Ge, J., Zhang, X., Liu, J., et al. Influence of capillary pressure boundary conditions and hysteresis on CO_2-water relative permeability. Fuel, 2022, 321: 124132.

Gorucu, S. E., Dang, C., Nghiem, L., et al. Modeling and optimization of low salinity waterflood with fines transport. Paper SPE 195901 Presented at SPE Annual Technical Conference and Exhibition, Calgary, Canada, 30 September-2 October, 2019.

Green, D. W., Willhite, G. P. Enhanced Oil Recovery. Texas, USA, Society of Petroleum Engineers, 1998.

Grolimund, D., Borkovec, M. Release of colloidal particles in natural porous media by monovalent and divalent cations. Journal of Contaminant Hydrology, 2006, 87(3): 155-175.

Guo, Z., Kang, N., Le-Hussain, F. An NMR-assisted laboratory investigation of coal fines migration in fracture proppants during single-phase water production. Fuel, 2023, 343: 127926.

Hao, J., Mohammadkhani, S., Shahverdi, H., et al. Mechanisms of smart waterflooding in carbonate oil reservoirs-A review. Journal of Petroleum Science and Engineering, 2019, 179: 276-291.

Hussain, F., Cinar, Y., Bedrikovetsky, P. A semi-analytical model for two phase immiscible flow in porous media honouring capillary pressure. Transport in Porous Media, 2012, 92: 187-212..

Hussain, F., Zeinijahromi, A., Bedrikovetsky, P., et al. An experimental study of improved oil recovery through fines-assisted waterflooding. Journal of Petroleum Science and Engineering, 2013, 109: 187-197.

Jerauld, G. R., Lin, C. Y., Webb, K. J., et al. Modeling low-salinity waterflooding. SPE Reservoir Evaluation & Engineering, 2008, 11(6): 1000-1012.

Katende, A., Sagala, F. A critical review of low salinity water flooding: Mechanism, laboratory and field application. Journal of Molecular Liquids, 2019, 278: 627-649.

Lager, A., Webb, K. J., Black, C. J. J., et al. Low salinity oil recovery-An experimental investigation1. Petrophysics-The SPWLA Journal of Formation Evaluation and Reservoir Description, 2008, 49(1): 28-35.

Lebedeva, E., J. Senden, T. J., Knackstedt, M., et al. Improved oil recovery from tensleep sandstone-Studies of brine-rock interactions by micro-CT and AFM. Paper Presented at 15th European Symposium on Improved Oil Recovery, Paris, France, 27-29 April, 2009.

Lemon, P., Zeinijahromi, A., Bedrikovetsky, P., et al. Effects of injected-water salinity on waterflood sweep efficiency through induced fines migration. Journal of Canadian Petroleum Technology, 2011, 50(9): 82-94.

Liu, C., Zhang, L., Li, Y., et al. Effects of microfractures on permeability in carbonate rocks based on digital core technology. Advances in Geo-Energy Research, 2022, 6(1): 86-90.

Martys, N. S., Hagedorn, J. G., Goujon, D., et al. Large-scale simulations of single-and multicomponent flow in porous media. Paper Presented at SPIE's International Symposium on Optical Science, Engineering, and Instrumentation, 18-23 July, 1999.

Moghadasi, R., Rostami, A., Hemmati-Sarapardeh, A. Application of nanofluids for treating fines migration during hydraulic fracturing: Experimental study and mechanistic understanding. Advances in Geo-Energy Research, 2019, 3(2): 198-206.

Mohammadi, M., Mahani, H. Direct insights into the pore-scale mechanism of low-salinity waterflooding in carbonates using a novel calcite microfluidic chip. Fuel, 2020, 260: 116374.

Mokhtari, R., Anabaraonye, B. U., Afrough, A., et al. Experimental investigation of low salinity water-flooding in tight chalk oil reservoirs. Journal of Petroleum Science and Engineering, 2022, 208: 109282.

Mokhtari, R., Ayatollahi, S., Fatemi, M. Experimental investigation of the influence of fluid-fluid interactions on oil recovery during low salinity water flooding. Journal of Petroleum Science and Engineering, 2019, 182: 106194.

Nande, S. B., Patwardhan, S. D. A review on low salinity waterflooding in carbonates: Challenges and future perspective. Journal of Petroleum Exploration and Production Technology, 2022, 12(4): 1037-1055.

RezaeiDoust, A., Puntervold, T., Strand, S., et al. Smart water as wettability modifier in carbonate and sandstone: A discussion of similarities/differences in the chemical mechanisms. Energy & Fuels, 2009, 23(9): 4479-4485.

Rivet, S. M., Lake, L. W., Pope, G. A. A coreflood investigation of low-salinity enhanced oil recovery. Paper SPE 134297 Prensented at SPE Annual Technical Conference and Exhibition, Florence, Italy, 19-22 September, 2010.

Sheng, J. J. Critical review of low-salinity waterflooding. Journal of Petroleum Science and Engineering, 2014, 120: 216-224.

Sohrabi, M., Mahzari, P., Farzaneh, S. A., et al. Novel insights into mechanisms of oil recovery by use of low-salinity-water injection. SPE Journal, 2017, 22(2): 407-416.

Tetteh, J. T., Brady, P. V., Barati Ghahfarokhi, R. B. Review of low salinity waterflooding in carbonate rocks: Mechanisms, investigation techniques, and future directions. Advances in Colloid and Interface Science 2020, 284: 102253.

Wang, Y., Almutairi, A. L. Z., Bedrikovetsky, P., et al. Insitu fines migration and grains redistribution induced by mineral reactions-Implications for clogging during water injection in carbonate aquifers. Journal of Hydrology, 2022, 614: 128533.

Wang, Y., Bedrikovetsky, P., Yin, H., et al. Analytical model for fines migration due to mineral dissolution during CO_2 injection. Journal of Natural Gas Science and Engineering, 2022, 100: 104472.

Wang, Z., Li, H., Lan, X., et al. Formation damage mechanism of a sandstone reservoir based on micro-computed tomography. Advances in Geo-Energy Research, 2021, 5(1): 25-38.

Wang, Y., Yu, M., Bo, Z., et al. Effect of temperature on mineral reactions and fines migration during low-salinity water injection into berea sandstone. Journal of Petroleum Science and Engineering, 2021, 202: 108482.

Yildiz, H. O., Morrow, N. R. Effect of brine composition on recovery of moutray crude oil by waterflooding. Journal of Petroleum Science and Engineering, 1996, 14(3): 159-168.

Yousef, A., Al-Saleh, S., Al-Jawfi, M. Improved/enhanced oil recovery from carbonate reservoirs by tuning injection water salinity and ionic content. Paper SPE 154076 Presented at SPE Improved Oil Recovery Symposium, Tulsa, Oklahoma, 2012.

Yu, M., Zeinijahromi, A., Bedrikovetsky, P., et al. Effects of fines migration on oil displacement by low-salinity water. Journal of Petroleum Science and Engineering, 2019, 175: 665-680.

Zahid, A., Shapiro, A., Skauge, A. Experimental studies of low salinity water flooding in carbonate reservoirs: A new promising approach. Paper SPE 155625 Presented at SPE EOR Conference at Oil and Gas West Asia, Muscat, Oman, 16-18 April, 2012.

Zeinijahromi, A., Lemon, P., Bedrikovetsky, P. Effects of induced fines migration on water cut during waterflooding. Journal of Petroleum Science and Engineering, 2011, 78(3): 609-617.

Zhang, L., Wang, Y., Miao, X., et al. Geochemistry in geologic CO_2 utilization and storage: A brief review. Advances in Geo-Energy Research, 2019, 3(3): 304-313.

Zhang, T., Li, Y., Li, C., et al. Effect of salinity on oil production: Review on low salinity waterflooding mechanisms and exploratory study on pipeline scaling. Oil & Gas Science and Technology-Revue d'IFP Energies nouvelles, 2020, 75: 50.